Received: 6 December 2019 | Revised: 3 June 2020 | Accepted: 23 June 2020

DOI: 10.1111/ajt.16183

AJT

ORIGINAL ARTICLE

DNA methylation modulates allograft survival and acute rejection after renal transplantation by regulating the mTOR pathway

Chaohong Zhu[1,2,3,4,5] | Wenyu Xiang[1,2,3,4,5] | Bingjue Li[1,2,3,4,5] | Yucheng Wang[1,2,3,4,5] | Shi Feng[1,2,3,4,5] | Cuili Wang[1,2,3,4,5] | Ying Chen[1,2,3,4,5] | Wenqing Xie[1,2,3,4,5] | Lihui Qu[1,2,3,4,5] | Hongfeng Huang[1,2,3,4,5] | Francesco Annunziata[6] | Suneetha Nunna[6] | Anna Krepelova[6] | Seyed Mohammad M. Rasa[6] | Francesco Neri[6] | Jianghua Chen[1,2,3,4,5] | Hong Jiang[1,2,3,4,5]

[1]Kidney Disease Center, the First Affiliated Hospital, College of Medicine, Zhejiang University, Hangzhou, Zhejiang, China

[2]Key Laboratory of Kidney Disease Prevention and Control Technology, Hangzhou, Zhejiang, China

[3]National Key Clinical Department of Kidney Diseases, Hangzhou, Zhejiang, China

[4]Institute of Nephrology, Zhejiang University, Hangzhou, Zhejiang, China

[5]The Third Grade Laboratory Under the National State, Administration of Traditional Chinese Medicine, Hangzhou, Zhejiang, China

[6]Leibniz Institute on Aging - Fritz Lipmann Institute (FLI), Jena, Thuringia, Germany

Correspondence
Hong Jiang
Email: jianghong961106@zju.edu.cn

Jianghua Chen
Email: zjukidney@zju.edu.cn

Acute rejection (AR) can lead to allograft dysfunction following renal transplantation, despite immunosuppressive treatments. Accumulating evidence points out a role for epigenetic modification in immune responses. However, the mechanism and contribution of DNA methylation in allograft survival remain unclear. In this study, we followed up patients who successively experienced end-stage renal disease, renal transplantation with allograft function or dysfunction, and hemodialysis. Peripheral blood mononuclear cells were collected at different time points for analysis of the DNA methylation. Epigenetic modifier analysis was also performed to explore its effect of methylation in a mouse model of AR. Compared with the allograft-stable cohort, patients who experienced AR-induced allograft dysfunction demonstrated more changes in methylation patterns. Pathway analysis revealed that the hypermethylated areas in the allograft dysfunction group were associated with genes related to the mechanistic target of rapamycin (mTOR) signaling pathway. Moreover, in the mouse AR model, treatment with the DNA methyltransferase inhibitor—decitabine regulated the Th1/2/17/regulatory T cell (Treg cell) immune response via its demethylating role in the suppressing the activity of the mTOR pathway, which ultimately ameliorated

Abbreviations: 1st Exon, first exon of genes; AKT1S1, AKT1 substrate 1; APC, allophycocyanin; AR, acute rejection; Bax, BCL2-associated X protein; Bcl2, B cell leukemia/lymphoma 2; Bcl2l1, BCL2-like 1; BSP, bisulfite sequencing PCR; CAB39, calcium-binding protein 39; Cdk, cyclin-dependent kinase; ChAMP, chip analysis methylation pipeline; CXCL, C-X-C-motif chemokine ligand; DDIT4, DNA damage inducible transcript 4; DEG, differentially expressed gene; DEPTOR, DEP domain containing mTOR interacting protein; DMR, differentially methylated region; DNMT, DNA methyltransferase; ESRD, end-stage renal disease; FDR, false discovery rate; FITC, fluorescein isothiocyanate; FOXP3, forkhead box P3; GATA, GATA-binding protein; H&E, hematoxylin and eosin; HRP, horseradish peroxidase; ICAMs, intercellular adhesion molecules; IFN, interferon; IGR, intergenic region; IL, interleukin; KEGG, Kyoto Encyclopedia of Genes and Genomes; MBD, methyl-CpG-binding domain; MCP, monocyte chemoattractant protein; mTOR, mechanistic target of rapamycin; MVP, methylation variable position; P70S6K, ribosomal protein S6 kinase B1; PAS, periodic acid-Schiff; PBMC, peripheral blood mononuclear cell; PCR, polymerase chain reaction; PE, phycoerythrin; PRKAB2, protein kinase AMP-activated non-catalytic subunit beta 2; PTEN, phosphatase and tensin homolog; Rheb, Ras homolog, mTORC1 binding; Rictor, RPTOR independent companion of mTOR, complex 2; RORC, RAR-related orphan receptor; Rptor, regulatory-associated protein of mTOR, complex 1; RT, renal transplantation; Runx3, runt-related transcription factor 3; SPSS, stroke-physiological saline solution; STK11, serine/threonine kinase 11; TET, Tet methylcytosine dioxygenase; TGF-β, transforming growth factor beta; Th cell, T helper cell; TNF, tumor necrosis factor; Treg cell, regulatory T cell; TSC2, tuberous sclerosis complex 2; TSS, transcription start site; UTR, untranslated region.

Chaohong Zhu and Wenyu Xiang contributed equally to this work.

Funding information
This work was supported by grants from the National Natural Science Foundation of China (No. 81470938 and 81770697).

renal allograft-related inflammatory injuries. These results revealed that changes in methylation accompany AR-induced allograft dysfunction after renal transplantation. Epigenetics may provide new insights into predicting and improving allograft survival.

KEYWORDS
basic (laboratory) research/science, clinical research/practice, genetics, graft survival, immunosuppressant – mechanistic target of rapamycin (mTOR), immunosuppression/immune modulation, kidney (allograft) function/dysfunction, kidney transplantation/nephrology, microarray array, rejection: acute

1 | INTRODUCTION

Renal transplantation (RT) is a highly effective and widely used treatment for end-stage renal disease (ESRD) that, compared to dialysis, provides patients with a better quality of life and significantly longer survival time (5-year adjusted survival for patients on dialysis vs transplantation: ~45% and ~92%, respectively).[1-3] Moreover, advances in immunosuppressive therapeutics have led to a substantial decline to <15% in the incidence of acute rejection (AR) within 1 year after RT.[4] However, AR events have reportedly increased in severity and thus continue to present a substantial risk of chronic allograft nephropathy and an obstacle for graft survival, as AR reduces overall graft survival by up to 24%.[4-7] Consequently, gaining an improved underlying AR can potentially minimize the risk and further improve the rate of overall long-term graft survival. Despite extensive effort, traditional genetic and current immunological approaches cannot thoroughly explain these anomalous findings, strongly suggesting the involvement of other biological mechanisms.

To address this issue, recent research initiatives have focused on integrative analyses of clinical/demographic data and bioinformatics data using network-based approaches, leading to the identification of latent mechanisms underlying disease-related processes.[8-10] Epigenetic modifications have aroused considerable attention in studies on several physiological and pathological processes owing to their intrinsic roles in normal cell development and function without altering the DNA sequence.[11-14] DNA methylation entails the addition of methyl groups to the 5′ position of cytosines through the activity of DNA methyltransferases (DNMTs), typically in the context of CpG-dinucleotide sites that are critical for gene transcriptional regulation.[15,16] Under specific conditions, methylation can be reprogrammed in cells, resulting in long-lasting effects even after the stimuli are removed.[17,18] Thereby, methylation has a dynamic capacity for flexible and inducible regulation of gene expression and has thus been traditionally considered as an "epigenetic clock."[16,19-22] Recent studies have shown that DNA methylation influences the activation, proliferation, differentiation, and migration of a variety of cell types implicated in allograft survival.[23-25] During $CD4^+$ T cell differentiation, DNA methylation was found to fix tissue-specific transcriptional patterns, thereby maintaining the original fate of differentiation while preventing differentiation by future generations of that lineage.[14] Similarly, DNMTs mediate the CpG methylation of specific regions that directly affect the differentiation of T helper (Th) 1/2 cells.[17,26] Moreover, demethylation of the RAR-related orphan receptor C (*RORC*) locus was reported to influence the phenotype of regulatory T (Treg) cells.[27] In contrast, demethylation events that enhance the expression of the forkhead box P3 (*FOXP3*) gene were associated with better allograft outcomes.[23,28] Furthermore, aberrant methylation also indirectly resulted in inflammatory injuries in diabetic kidneys by influencing the mechanistic target of rapamycin (mTOR) signaling pathway.[29] Although this preliminary work has explored the effects of epigenetic modification on the immune response, the relationship between DNA methylation and AR after renal transplantation or AR-induced allograft dysfunction remains to be clarified.

Considering that epigenetics is an emerging field of research in kidney transplantation, we hypothesized that DNA methylation patterns would be modified after organ transplantation accompanied by abnormal expression of some specific genes, which would then activate the immune-associated signaling pathway, further influence the differentiation of T cells, and finally manipulate the fate of allografts. To test this hypothesis, we used a whole-genome bisulfite sequencing approach to compare the methylation patterns in transplant recipients with and without AR. We further conducted bioinformatics to examine the genes associated with hypermethylated regions and their functions. Moreover, we established a mouse model of AR that was treated with a DNA methylation inhibitor to examine the impact of methylation on allograft survival and tolerance.

2 | MATERIALS AND METHODS

2.1 | Blood sample collection and processing

All blood samples were collected from the kidney transplant and hemodialysis wards of the Kidney Disease Center, First Affiliated Hospital, College of Medicine, Zhejiang University. Written and informed consent was provided by all patients who received the donor kidney and underwent the renal transplantation. Peripheral blood mononuclear cells (PBMCs) were isolated from heparinized blood and then preserved in cell culture freezing medium at −80°C in the

biobank. Renal biopsy samples from all consenting patients were also collected and stored in the biobank. The study was approved by the local research ethics committee.

2.2 | Experimental design

The study design is schematically described in Figure 1, and clinical characteristics of patients are summarized in Table S1. Group 1 consisted of a patient cohort with AR-induced allograft dysfunction, from whom blood was collected at the following time points: (a) during ESRD but before transplantation, (b) upon loss of function of the grafted kidneys, and (c) after patients had undergone an average of 3 years of hemodialysis following allograft dysfunction. Group 2 was composed of the graft-stable cohort, from whom blood was collected at the following time points: (a) during ESRD but before transplantation, (b) following transplantation when the grafted kidneys functioned normally, and (c) at a later stage during which the grafted kidneys continued to function normally. Group 3 included samples obtained from a cohort of 13 healthy individuals. All patients in Group 1 had suffered from AR (T cell–mediated rejection) prior to allograft failure. None of the patients in Group 2 had a history of AR. The details of the recipients' diagnosis and therapy are provided in Supplemental Methods - Additional information about the recruited patients.

2.3 | Bisulfite-converted DNA preparation and methylation sequencing

Genomic DNA was extracted from PBMCs using an AxyPrep blood genomic DNA maxiprep kit (Axygen; Corning Inc, Tewksbury, MA). After assessing the DNA quality, purity, and integrity, the extracted DNA was bisulfite-converted using an EpiTect bisulfite kit (Qiagen, Hilden, Germany) and then applied to microarray or bisulfite sequencing polymerase chain reaction (PCR) for analysis of DNA methylation. The details of sequencing procedures and data analysis are provided in Supplemental Methods - Microarray and bisulfite sequencing PCR (BSP) for DNA methylation analysis.

2.4 | Establishment of a mouse AR model of renal transplantation

Ectopic renal transplantation was performed according to previously reported microsurgical techniques.[30] Kidneys from male BALB/c mice (H-2d; 8 weeks old) were transplanted into C57BL/6 mice (H-2b; 8 weeks old) mice. Half of the C57BL/6 recipients received decitabine (1.5 mg/kg per day)[31] by intraperitoneal injection starting from the day after transplantation, whereas the others received stroke-physiological saline solution (SPSS; isometric). The animal experiments were performed in accordance with institutional guidelines approved by the Animal Use Committee of Zhejiang University. The grafted kidneys and spleens from recipient mice were procured on day 7 after transplantation, part of which were used for hematoxylin and eosin staining or periodic acid-Schiff staining for histopathologic assessment. The unstained sections of mouse grafted kidneys and human renal allograft biopsies were incubated with anti-CD3 antibody (Abcam, Cambridge, UK) and DNMT1 (Novus Biologicals, Littleton, CO) for immunological staining following standard protocols.

2.5 | Flow cytometry analysis

The grafted kidneys and spleens were digested and then filtered using a 40-μm cell strainer into single-cell suspensions. After enrichment, the immune cells were stimulated by Cell Stimulation Cocktail with protein transport inhibitors (eBioscience, San Diego, CA) for 6 hours in a CO_2 incubator. In brief, 5×10^6 cells in 100 μL of staining

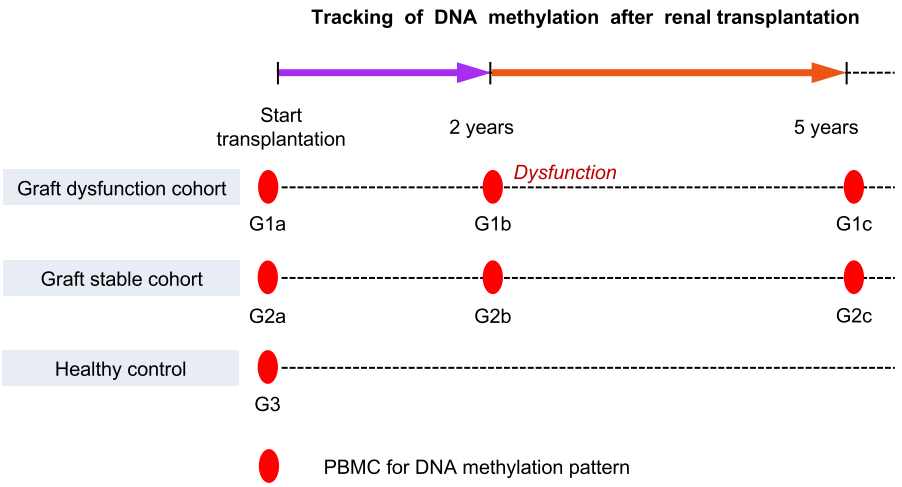

FIGURE 1 Description of the study cohorts. Schematic diagram of the study cohorts identifying dynamic changes in DNA methylation patterns to explore their potential influence. PBMC, peripheral blood mononuclear cell

FIGURE 2 DNA methylation analysis of target CpG sites from the allograft dysfunction group. A, Flow diagram of target differentially methylated CpG sites from the intersection of Groups 1a vs 1b and Groups 1b vs 1c. B, Volcano plot of these target CpG sites in the comparison of Groups 1a and 1b. Dark blue/red: FDR < 0.05. C, Genome-wide differential methylation status for the target CpG sites. Differences in methylation status (Δbeta) of all CpG sites that passed Bonferroni correction are plotted. Red dots represent Δbeta < 0; blue dots represent Δbeta > 0. Chromosomes are shown clockwise from 1 through 22, except for chromosomes X and Y. D, RefSeq annotations of the target MVPs. Enrichment ratio of the MVP relative to representation of the different elements on the methylation microarray. FDR < 0.05 according to the Benjamini-Hochberg procedure. Proximal promoters were defined as 200 bp (TSS200) or 1500 bp (TSS1500) upstream of the transcription start site. E, Violin plot representation of methylation levels of the target CpG sites from Groups 1 and 2 with hypermethylated MVPs (left) and hypomethylated MVPs (right). Solid lines represent the global DNA methylation levels in Groups 1 and 2. FDR, false discovery rate; MVP, methylation variable position; TSS, Transcription start site

buffer were incubated with CD3-PE-Cyanine7 and CD8-fluorescein isothiocyanate (FITC) antibodies, followed by fixation, permeabilization, and incubation with anti-interferon (IFN)-γ-allophycocyanin (APC), anti-interleukin (IL)-4-phycoerythrin (PE), anti-Foxp3-APC, and anti-IL-17α-PE antibodies (eBioscience). Finally, the stained cells were analyzed using a Cytoflex flow cytometer (Beckman Coulter, Brea, CA).

2.6 | Gene expression analysis

Total RNA was extracted using Trizol reagent (Invitrogen, Carlsbad, CA) and reverse-transcribed to cDNA using a reverse transcription kit (TaKaRa, Mountain View, CA). Real-time PCR was performed using SYBR Green qPCR master mix (Vazyme Biotech, Nanjing, China) on a ViiA7 Real-Time PCR system (Applied Biosystems, Foster City, CA). Primer sequences for real-time PCR are provided in Table S7.

2.7 | Western blot

Proteins from the grafted kidneys were extracted and then used for separation and transfer. The membranes were blocked and then incubated with primary antibodies against T-bet, GATA3, Foxp3, RORγt (Abcam), DNMT1 (Novus Biologicals), p-Akt, p-mTOR, p-P70S6K, PTEN (Cell Signaling Technology, Danvers, MA), DDIT4, and GAPDH (Proteintech, Rosemont, IL). After washing, the membranes were incubated with horseradish peroxidase (HRP)-conjugated secondary antibodies and subsequently washed again. Chemiluminescence signals were detected after exposure to Immobilon Forte Western HRP substrate (EMD Millipore, Burlington, MA) using the ChemiDocTM XRS+System (Bio-Rad, Hercules, CA).

2.8 | Statistical analysis

The analytical details of methylation data are provided in the Supplemental Methods - Analysis of methylation data. Data are expressed as the mean ± SEM, unless otherwise indicated, and were analyzed with GraphPad Prism 8.0 (GraphPad Software, Inc, La Jolla, CA) using a *t* test, one-way analysis of variance followed by Tukey's post hoc test, chi-square test, and Mann-Whitney *U* test as appropriate. A $P < .05$ was defined as significant.

3 | RESULTS

3.1 | Significantly different genome-wide methylation patterns between PBMCs from patients with AR-induced allograft dysfunction group

To account for potential differences in genetic background among patients in this study, PBMC samples were collected at the time of transplant (day 0), corresponding to a mean of 27.2 ± 3.68 months before allograft dysfunction. The basal methylation levels observed at this time point were then used as a basis for comparison between time points and between groups. Comparison of Groups 1a and 1b revealed 432,695 CpG sites that passed quality filtering, with 27 772 different sites (false discovery rate <0.05) corresponding to 11 039 genes, indicating substantial differences in methylation from pre-transplant until allograft dysfunction. In contrast, no differences in methylation were found in comparative analysis of Groups 2a and 2b (Figure S1E,F), suggesting that the differences in methylation between the Group 1a and 1b were related to the dysfunction of the renal transplant. When Group 1 patients had to receive the hemodialysis after allograft dysfunction, some specifically sensitive CpG sites would be altered. Finally, 10 648 target CpG sites were screened out by the intersections of Group 1a vs 1b and Group 1b vs 1c (Figure 2A).

Among these target CpG sites, 1683 CpG sites were hypermethylated and 8965 CpG sites were hypomethylated (Figure 2B). The total annotated CpG sites with significantly different methylation between groups were distributed across the genome, with most sites located on Chr1, Chr2, and Chr6 (Figure 2C and Table S2). To focus on the potential roles of methylation in gene regulation, we screened these target CpG sites resulting in the identification of sites within TSS1500 (16.61%), TSS200 (7.22%), 5′ untranslated regions (UTRs; 9.75%), the first exon of genes (1st Exon; 2.81%), the gene body (Body; 36.26%), 3′ UTRs (3.9%), and intergenic regions (IGRs; 23.45%), while they were also distributed across the island (13.31%), shore (29.56%), shelf (12.13%), and open sea (44.99%) (Figure 2D and Table S3). This distinct pattern of genome-wide methylation showed that the highest methylation rates were in gene body regions, and the lowest were in 1st Exon regions. Moreover, these target CpG site were also tracked in the Groups 1 and 2. Notably, there were greater differences observed between Groups 1a and 1b than between Groups 2a and 2b, although these parallel comparisons showed similar trends in variation (Figure 2E).

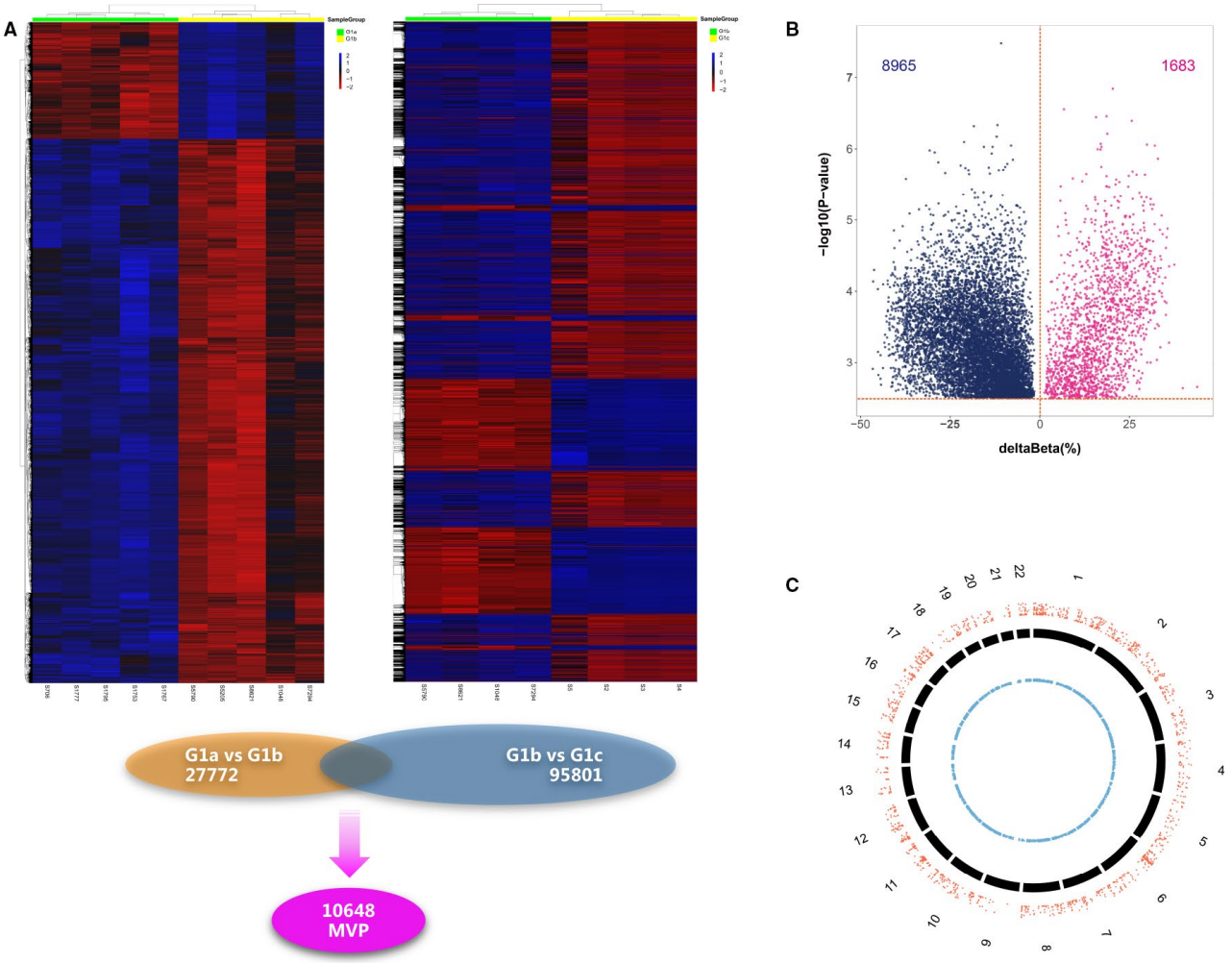
A
B
8965
1683
−log10(P−value)
deltaBeta(%)
C
G1a vs G1b
27772
G1b vs G1c
95801
10648
MVP
D
TSS1500
TSS200
5'UTR
1st Exon
Body
3'UTR
IGR
16.6%
7.2%
9.7%
2.8%
36.3%
3.9%
23.5%
Island
Shore
Shelf
Open sea
13.3%
29.6%
12.1%
45%
E
Hyper.MVP
Hypo.MVP
beta value
G1a
G1b
G2a
G2b

FIGURE 3 Enrichment analysis of DMRs identified in allograft dysfunction patients. A, Enrichment of DEGs with hypermethylated/hypomethylated DMRs in Group 1. B, GO analysis of DEGs with hypermethylated DMRs in Group 1. C, MethPrimer indicated the distribution of CpG sites in the promoter region of *RUNX3*. D, The delta β value of each CpG site in this DMR (*RUNX3*, chr1: 25290947-25292412, overlapped with the gene promotor) of Group 1a vs Group 1b as compared with the corresponding CpG sites in the same region of Group 2a vs Group 2b from the Infinium HumanMethylation450 BeadChip. E, The delta β value of each CpG site of the target DMR (*RUNX3*, chr1: 25291385-25291584, overlapped with 1st Exon and TSS200) verified by bisulfite sequencing PCR with additional human peripheral blood mononuclear cell (PBMC) samples from the graft dysfunction/stable group. BSP, bisulfite sequencing PCR; DEG, differentially expressed gene; DMR, differentially methylated region; GO, gene ontology; KEGG, Kyoto Encyclopedia of Genes and Genomes; PCR, polymerase chain reaction; RUNX3, runt-related transcription factor 3

3.2 | Hypermethylation of immune-related signaling genes associated with differentially methylated regions (DMRs) identified in allograft dysfunction patients

We evaluated the possible biological effects of DNA methylation by examining DNA regions that are prone to methylation and represent methylation-regulated genes, using ChAMP[32] to identify significant DMRs in each experimental group. A total of 1021 DMRs were identified between Groups 1a and 1b that mapped to 917 unique genes. Kyoto Encyclopedia of Genes and Genomes (KEGG) enrichment analysis was then conducted to assess the potential biological relevance of the significantly hypermethylated or hypomethylated DMRs (Figure 3A). Group 1 hypermethylated genes were enriched for T cell receptor and mechanistic target of rapamycin signaling pathways, which were not found among Group 1 hypomethylated genes or among any of the Group 2 DMRs (Figure 3A; Figure S2). DAVID analysis and visualization with the enrichment map, gene ontology terms clustering for "T cell" were indicated as the major category of differentially hypermethylated genes (Figure 3B). Combined with the fact that patients in Group 1 had a history of T cell–mediated rejection prior to allograft failure, these findings suggested that hypermethylation of these regions was associated with AR-induced allograft dysfunction.

3.3 | The Runt-related transcription factor 3 *(RUNX3)* promoter region is the most hypermethylated DMR in patients with allograft dysfunction

Among the hypermethylated DMRs identified between Group 1a and Group 1b, the DMR with the highest incidence of methylation involved the promoter of *RUNX3*, an essential gene involved in the immune response.[33,34] Each CpG site in this methylated region (*RUNX3*, chr1: 25290947-25292412) overlapped with the gene promoter (Figure 3C and Table S4). Reanalysis of this region using microarray data showed that the average of delta β value for all CpG sites in this DMR between Groups 1a and 1b (0.2147) was almost twice that between Group 2a vs Group 2b (0.0978) (Figure 3D). After viewing this methylated region in the Integrative Genomics Viewer, a smaller target methylated region was selected for closer scrutiny (*RUNX3*, chr1: 25291385-25291584), which overlapped with the 1st Exon and TSS200 regions (Figure 3C; Figure S3). To verify the hypermethylation of this target region, bisulfite sequencing PCR (BSP) and additional human PBMC samples from graft dysfunction/stable cohorts were analyzed, revealing that this target region was indeed much more hypermethylated in the graft dysfunction cohort than in the graft-stable cohort (Figure 3E), which confirmed our previous conclusions that allograft dysfunction patients have more hypermethylation than graft-stable recipients. Therefore, methylation can be considered as an indicator for monitoring allograft function after transplantation. Recent studies have found that *RUNX3* was a negative regulator in the mTOR signaling pathway.[35,36] Furthermore, the mTOR signaling pathway emerged in the KEGG enrichment analysis of hypermethylated DMRs. Therefore, we next assessed the role of DNA methylation in the mTOR signaling pathway in allograft rejection.

3.4 | DNA methylation inhibitor ameliorates renal allograft inflammatory injuries

To investigate whether inhibition of DNA methylation can alleviate graft rejection, the effects of decitabine treatment on DNA methylation were explored in a mouse AR model of renal transplantation. Compared with the SPSS-treated group, histological analyses revealed the development of milder AR of the renal allograft with much less infiltration of $CD3^+$ cells in decitabine-treated mice (Figure 4A). Moreover, the renal allografts in decitabine-treated mice showed a reduction in the severity of allograft rejection and relatively lower levels of creatinine and the proinflammatory cytokines *Cxcl9*, *Icam1*, *Il6*, *Mcp1*, *Tnfa*, and *Tgfβ* (Figure 4B,C; Figure S4A). Therefore, the affected genes modulate T cell recruitment and differentiation and ultimately lead to the infiltration of inflammatory cells and allograft pathological impairment.

3.5 | Decitabine influenced the infiltration of immune cells

In light of previous findings, the Th1 and Th2 cell immune responses to the grafted donor kidney were examined in decitabine- and SPSS-treated mice. Flow cytometry analysis revealed a 6.03% reduction in Th1 cells relative to levels in SPSS-treated mice, demonstrating that decitabine treatment suppressed the Th1-specific immune response in the grafted kidney. By contrast, the Th2-specific immune response was attenuated in the grafted kidneys from decitabine-treated mice, although only by a 1.1% decrease in Th2 cells compared to that in

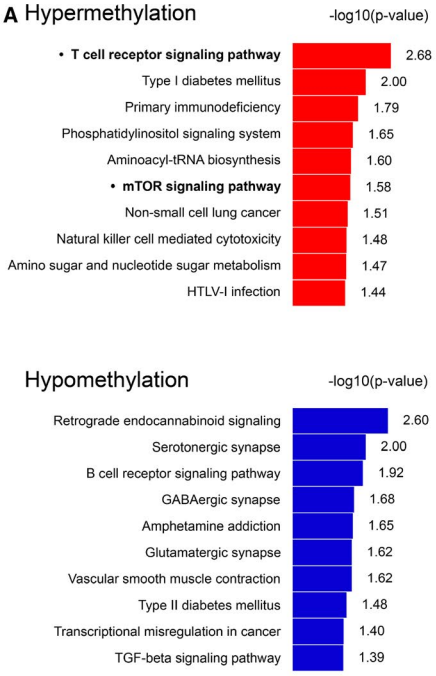
A Hypermethylation
-log10(p-value)
• T cell receptor signaling pathway 2.68
Type I diabetes mellitus 2.00
Primary immunodeficiency 1.79
Phosphatidylinositol signaling system 1.65
Aminoacyl-tRNA biosynthesis 1.60
• mTOR signaling pathway 1.58
Non-small cell lung cancer 1.51
Natural killer cell mediated cytotoxicity 1.48
Amino sugar and nucleotide sugar metabolism 1.47
HTLV-I infection 1.44
Hypomethylation
-log10(p-value)
Retrograde endocannabinoid signaling 2.60
Serotonergic synapse 2.00
B cell receptor signaling pathway 1.92
GABAergic synapse 1.68
Amphetamine addiction 1.65
Glutamatergic synapse 1.62
Vascular smooth muscle contraction 1.62
Type II diabetes mellitus 1.48
Transcriptional misregulation in cancer 1.40
TGF-beta signaling pathway 1.39

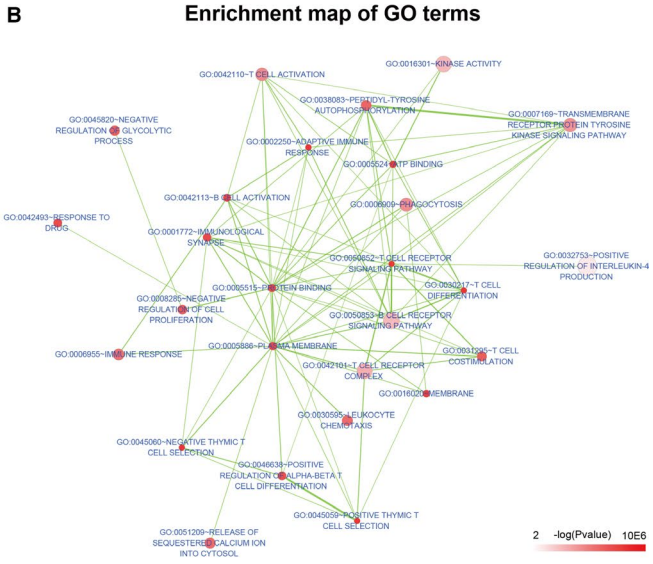
B
Enrichment map of GO terms
GO:0016301~KINASE ACTIVITY
GO:0042110~T CELL ACTIVATION
GO:0038083~PEPTIDYL-TYROSINE AUTOPHOSPHORYLATION
GO:0007169~TRANSMEMBRANE RECEPTOR PROTEIN TYROSINE KINASE SIGNALING PATHWAY
GO:0045820~NEGATIVE REGULATION OF GLYCOLYTIC PROCESS
GO:0002250~ADAPTIVE IMMUNE RESPONSE
GO:0005524~ATP BINDING
GO:0042113~B CELL ACTIVATION
GO:0006909~PHAGOCYTOSIS
GO:0042493~RESPONSE TO DRUG
GO:0001772~IMMUNOLOGICAL SYNAPSE
GO:0032753~POSITIVE REGULATION OF INTERLEUKIN-4 PRODUCTION
GO:0050852~T CELL RECEPTOR SIGNALING PATHWAY
GO:0030217~T CELL DIFFERENTIATION
GO:0008285~NEGATIVE REGULATION OF CELL PROLIFERATION
GO:0050853~B CELL RECEPTOR SIGNALING PATHWAY
GO:0006955~IMMUNE RESPONSE
GO:0031295~T CELL COSTIMULATION
GO:0042101~T CELL RECEPTOR COMPLEX
GO:0030595~LEUKOCYTE CHEMOTAXIS
GO:0045060~NEGATIVE THYMIC T CELL SELECTION
GO:0046639~POSITIVE REGULATION OF ALPHA-BETA T CELL DIFFERENTIATION
GO:0045059~POSITIVE THYMIC T CELL SELECTION
GO:0051209~RELEASE OF SEQUESTERED CALCIUM ION INTO CYTOSOL
2 -log(Pvalue) 10E6

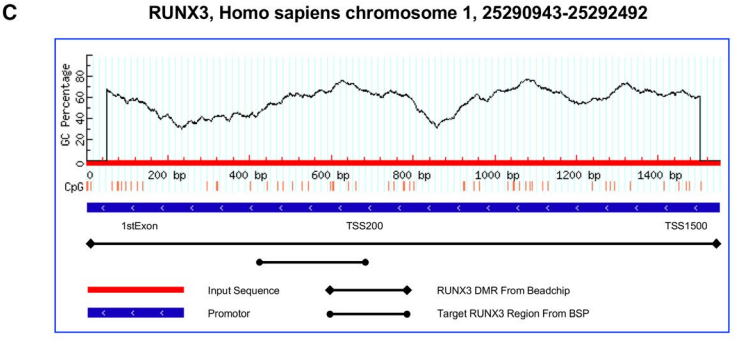
C
RUNX3, Homo sapiens chromosome 1, 25290943-25292492
GC Percentage
0 20 40 60 80
0 200 bp 400 bp 600 bp 800 bp 1000 bp 1200 bp 1400 bp
CpG
1stExon
TSS200
TSS1500
Input Sequence
Promotor
RUNX3 DMR From Beadchip
Target RUNX3 Region From BSP

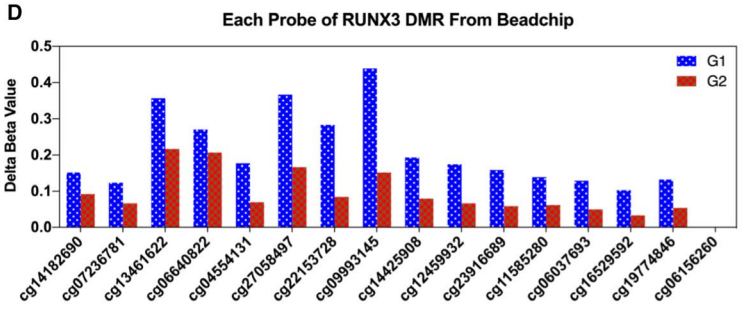
D
Each Probe of RUNX3 DMR From Beadchip
Delta Beta Value
0.0 0.1 0.2 0.3 0.4 0.5
G1
G2
cg14182690
cg07236781
cg13461622
cg06640822
cg04554131
cg27058497
cg22153728
cg09993145
cg14425908
cg12459932
cg23916689
cg11585280
cg06037693
cg16529592
cg19774846
cg06156260

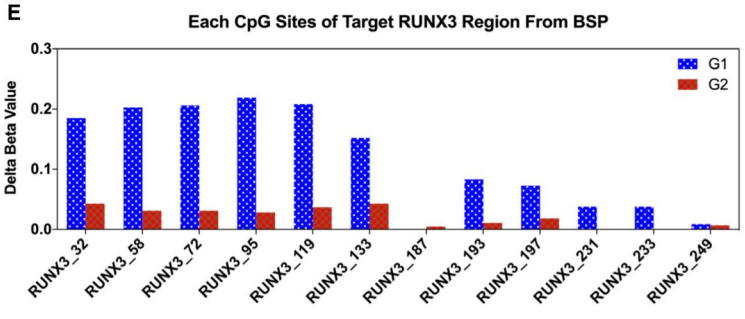
E
Each CpG Sites of Target RUNX3 Region From BSP
Delta Beta Value
0.0 0.1 0.2 0.3
G1
G2
RUNX3_32
RUNX3_58
RUNX3_72
RUNX3_95
RUNX3_119
RUNX3_133
RUNX3_187
RUNX3_193
RUNX3_197
RUNX3_231
RUNX3_233
RUNX3_249

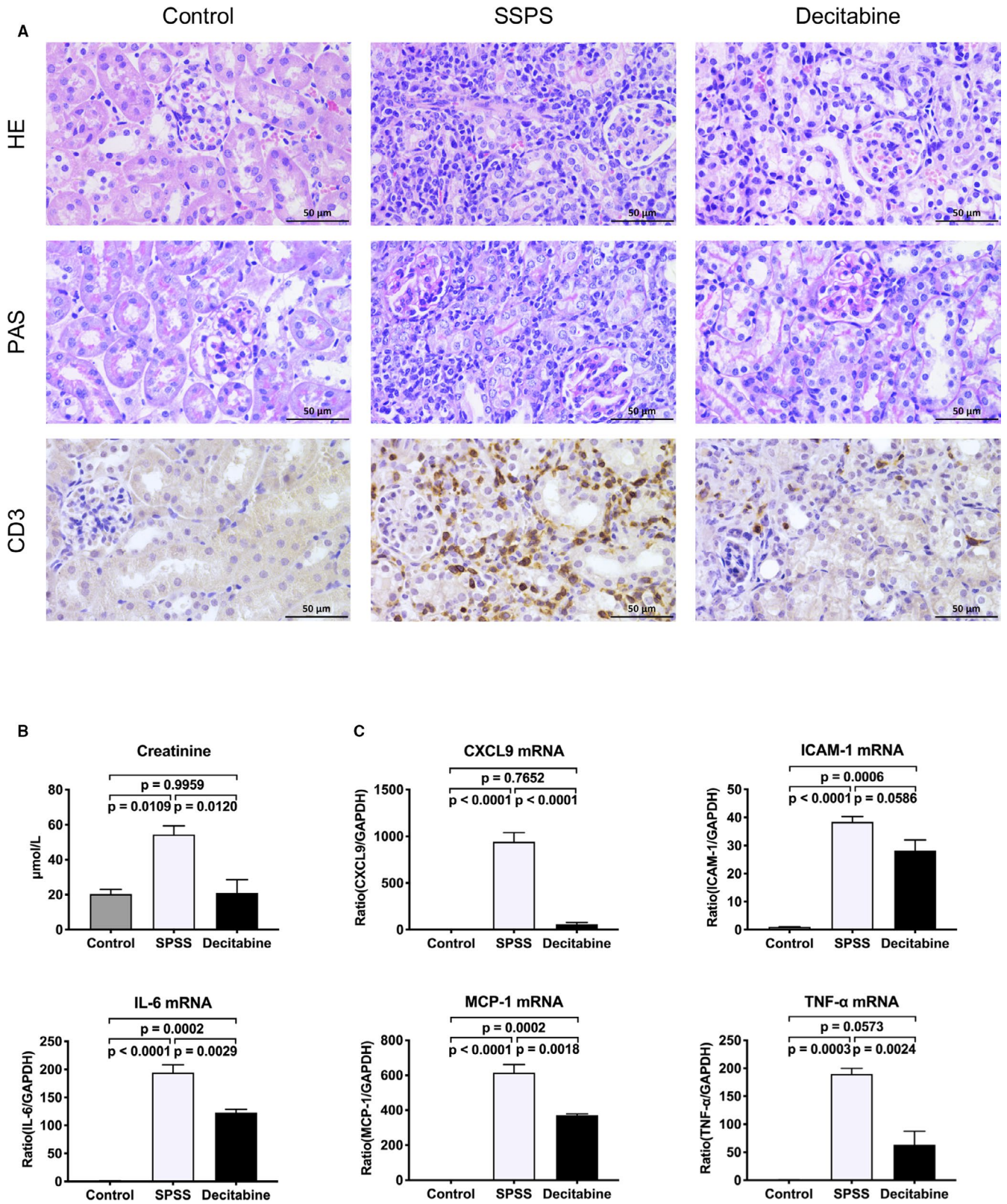

FIGURE 4 Decitabine treatment significantly ameliorates renal allograft rejection. A, H&E, PAS, and immunohistochemistry (CD3) staining show the histopathological changes in renal allografts on postoperative day 7. Scale bar = 50 μm. B, Creatinine levels at 7 d after renal transplantation. C, Real-time PCR to determine the mRNA levels (*Cxcl9*, *Icam1*, *Il6*, *Mcp1*, and *Tnfa*) in renal allografts on postoperative day 7. Data are expressed as the mean ± SEM. BSP, bisulfite sequencing PCR; CXCL, C-X-C-motif chemokine ligand; DMR, differentially methylated region; H&E, hematoxylin and eosin; ICAM-1, intercellular cell adhesion molecule-1; IL, interleukin; MCP, monocyte chemoattractant protein; PAS, periodic acid-Schiff; PCR, polymerase chain reaction; SPSS, stroke-physiological saline solution; TGF, transforming growth factor; TNF, tumor necrosis factor

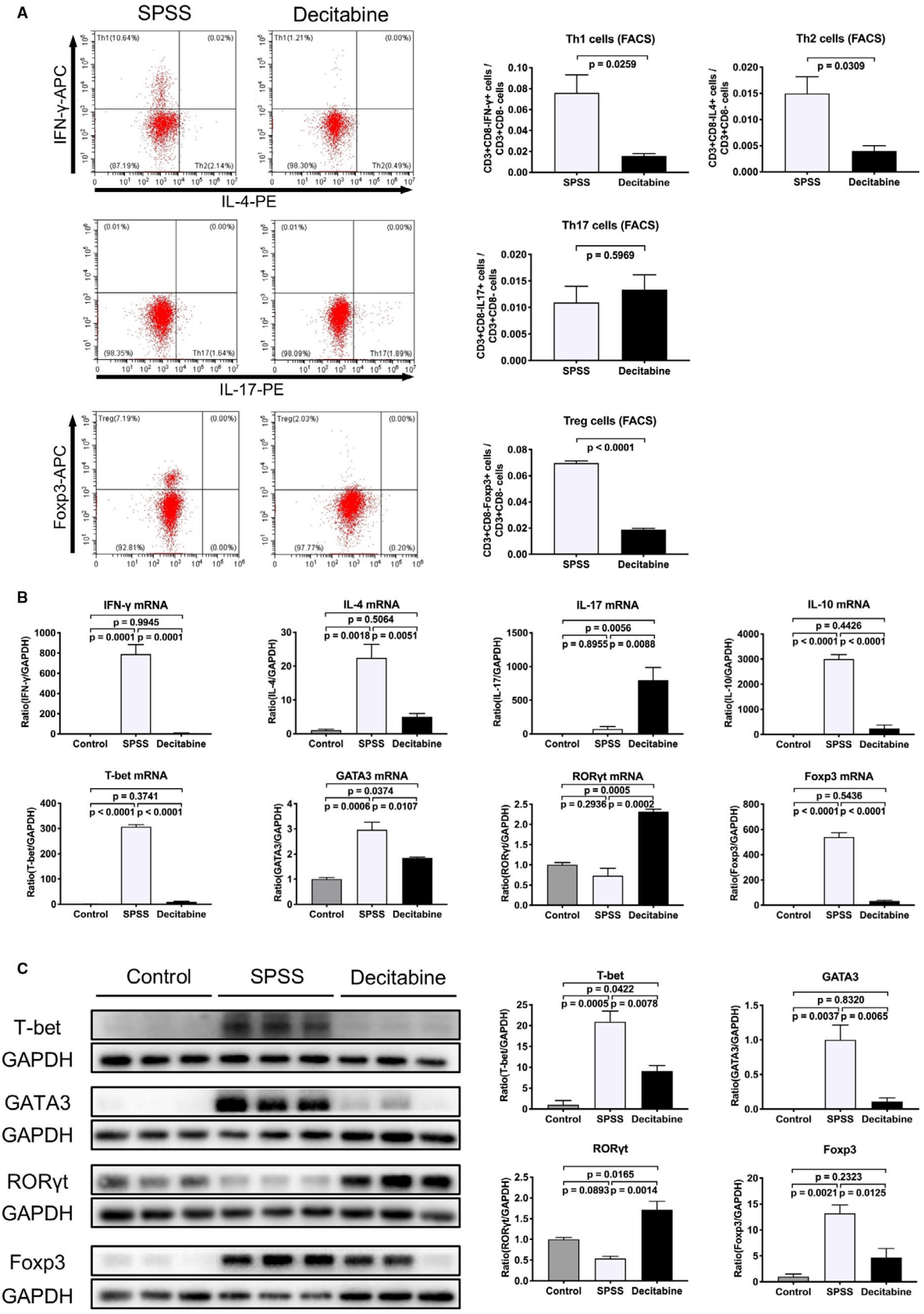

SPSS-treated mice (Figure 5A), which was further validated by quantitative PCR and western blot analysis (Figure 5B,C). These results suggested that decitabine repressed the Th1/2 immune response during acute allograft rejection, which was consistent with the observed systematic pattern of T cell differentiation, such as the similar decrease in Th1/2 levels in the spleen following decitabine treatment (Figure S5).

FIGURE 5 Decitabine treatment significantly regulates Th1/2/17 and Treg cell infiltration during renal allograft rejection. A, Quantitative analysis of Th1 ($CD3^+CD8^-IFN\text{-}\gamma^+$), Th2 ($CD3^+CD8^-IL\text{-}4^+$), Th17 ($CD3^+CD8^-IL\text{-}17^+$), and Treg ($CD3^+CD8^-Foxp3^+$) cells according to three-color flow cytometry using renal allografts from SPSS- or decitabine-treated recipient mice on postoperative day 7. B, Quantitative polymerase chain reaction analysis of Th1 (*Ifng* and *Tbet*), Th2 (*Il4* and *Gata3*), Th17 (*Il17* and *Rorgt*) and Treg (*Il10* and *Foxp3*) levels in renal allografts. C, Western blot analysis of T-bet, GATA3, RORγt, and FOXP3 levels in renal allografts. Data are expressed as the mean ± SEM. Foxp3, forkhead box P3; GATA, GATA-binding protein; IFN, interferon; PCR, polymerase chain reaction; RORγt, RAR-related orphan receptor; SPSS, stroke-physiological saline solution; Th, T helper cell; Treg, regulatory T cell

Likewise, we analyzed the effect of decitabine on Th17-mediated immune responses. Flow cytometry analysis showed no obvious difference of Th17 cells in the donor kidneys, and even reduction in the spleens, from decitabine-treated mice, in contrast to those of SPSS-treated mice (Figure 5A; Figure S5). However, quantitative PCR and western blot analysis revealed that the expression levels of Th17-associated cytokine (IL-17) and transcription factor (RORγt) were enhanced (Figure 5B,C). Furthermore, analysis of Treg-mediated responses displayed a significant reduction in Treg cells, which was consistent with quantitative PCR and western blot analysis (Figure 5; Figure S5). These results showed that chemical suppression of DNA methylation can mitigate the T helper cell–mediated immune response to renal allografts.

3.6 | Decitabine controlled the activity of the mTOR pathway

Investigation of the regulatory effect of a DNA methylation inhibitor on the mTOR signaling pathway demonstrated that the expression of DNMT1 was downregulated in the allografted kidney (Figure 6A,C). Quantitative PCR analysis showed that mRNA levels of *Akt1s1*, *Ddit4*, *Deptor*, *Pten*, and *Tsc2*, negative regulators of the mTOR pathway, were increased (Figure 6B). These results were consistent with the findings in the recipient spleens (Figure 7). Similar to the finding of the hypermethylation of *RUNX3* in the allograft dysfunction cohort, the sequencing data displayed that *Runx3*, *Ddit4*, and *Pten* showed lower methylation levels in the promotor and higher mRNA expression levels with the treatment of decitabine (Figure 6B; Figures S7-S9). However, the methylation level of the intron region of *Foxp3* and mRNA levels of *Akt*, *mTor*, *Rheb*, *Rictor*, and *Rptor* were not significantly changed (Figures S4B and S10). Consequently, the phosphorylation of AKT was inhibited, leading to suppressed activity of the downstream signal molecules, including the p-mTOR and p-P70S6K (Figures 6C and 7C).

Considering that the mTOR signaling pathway affects the cell cycle progression, a series of cell cycle–related factors were explored in the recipient spleens. Quantitative PCR demonstrated that the mRNA levels of cell cycle inhibitors (*p21*, *p27*, but not *p15*) were enhanced in the decitabine-treated group. By contrast, other cell proliferation–related factors, including Cyclin A, Cyclin B, Cyclin D, and Ki-67, were repressed in recipients with the treatment of decitabine (Figure S6B).

Two-color immunofluorescence analysis revealed that the grafted kidneys with acute rejection contained large numbers of DNMT1-expressing $CD3^+$ T cells in contrast to those with no or only a mild inflammatory response (Figure 8). In summary, mTOR pathway inhibition influenced the immune response of Th 1/2/17 and Treg cells. These results further demonstrated that decitabine regulated T cell–mediated allograft rejection via its demethylating role in the mTOR pathway.

4 | DISCUSSION

Substantial research has been undertaken to improve allograft survival; however, allograft injuries caused by immune responses remains a major challenge. Epigenetic modulation of expression of immune system-related genes can dynamically regulate innate and adaptive immune responses[37] and ultimately introduces several vulnerabilities to allograft survival. Therefore, methylation can be an important potential marker for allograft outcome. However, gaining a better understanding of methylation activity after transplantation is necessary, especially given the current limitations of our understanding about the impact of epigenetic modification in organ transplantation.

Data generated by our comparative DNA microarray suggested that AR-induced allograft dysfunction was associated with changes of hypermethylation in allograft recipients and pathway enrichment analysis of the DMRs showed that hypermethylated genes were primarily involved in immune-related signaling pathways (including the mTOR pathway). Subsequent bisulfite sequencing PCR analysis further validated that DNA hypermethylation was indeed present in the AR-induced allograft dysfunction cohort. Thus, we hypothesized that administration of DNA methylation inhibitors could potentially ameliorate AR-induced allograft dysfunction.

Using an in vivo mouse model of AR, decitabine treatment decreased the DNMT1 expression level in recipients with a subsequent increase in the level of mTOR upstream negative regulators, ultimately repressing the activity of the mTOR signaling pathway, which was consistent with the findings of Chen et al.[29] Delgoffe et al[38] reported that mTOR pathway inhibition enhanced the expression of SOCS3, which negatively regulated the STAT4 signaling and inhibited Th1 differentiation. Although the repressed mTOR pathway could increase STAT4 phosphorylation and GATA3 expression to drive Th2 differentiation, Lee et al[39] found that Th2 cell differentiation was still controlled by other vital determinants (such as protein kinase C). These findings indicated that multiple signaling pathways participated in Th2 cell differentiation.

Although inhibition of mTOR pathway could induce Treg development, Treg cells were still reduced after decitabine treatment. Our results demonstrated that transforming growth factor beta (TGF-β) expression was significantly downregulated in decitabine-treated group,

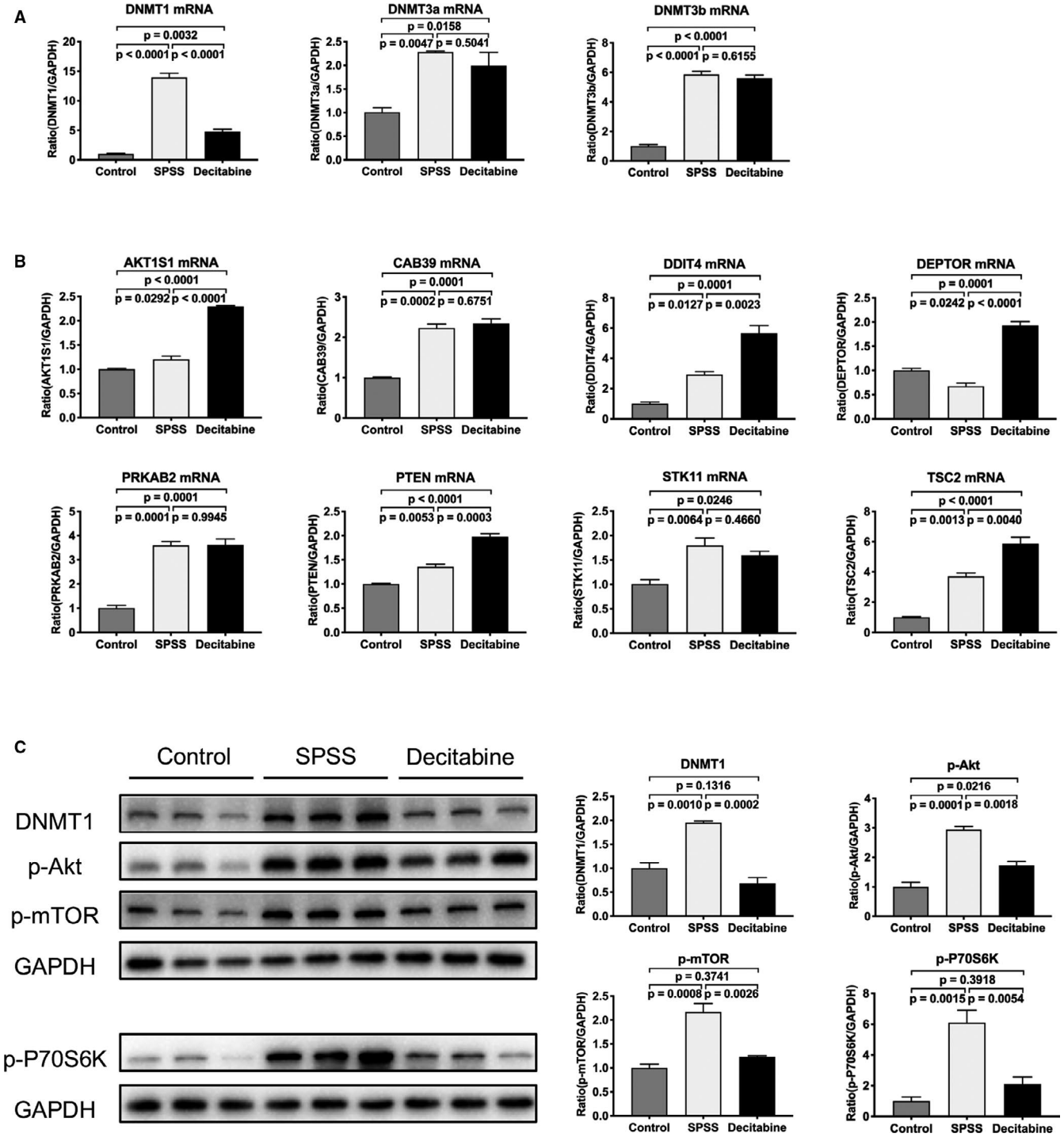

FIGURE 6 Decitabine treatment modulates the mTOR signaling pathway during renal allograft rejection. A, Quantitative PCR analysis of *Dnmt1/3a/3b* from renal allografts on postoperative day 7. B, Quantitative PCR analysis of *Akt1s1*, *Cab39*, *Ddit4*, *Deptor*, *Prkab2*, *Pten*, *Stk11*, and *Tsc2* mRNA expression from renal allografts. C, Western blot analysis of DNMT1, p-AKT, p-mTOR, and p-70S6K from renal allograft. Data are expressed as the mean ± SEM. AKT1 substrate 1; CAB39, calcium-binding protein 39; DDIT4, DNA damage inducible transcript 4; DEPTOR, DEP domain containing mTOR interacting protein; DNMT, DNA methyltransferase; AKT1S1, mTOR, mechanistic target of rapamycin; PCR, polymerase chain reaction; PRKAB2, protein kinase AMP-activated non-catalytic subunit beta 2; PTEN, phosphatase and tensin homolog; SPSS, stroke-physiological saline solution; STK11, Serine/threonine kinase 11; TSC2, tuberous sclerosis complex 2

and impairment of TGF-β signaling was previously demonstrated to affect the Treg response.[40] Kim et al[41] confirmed that the methylation level of the first intron of *Foxp3* decreased, subsequently promoting Treg differentiation. However, we did not find a significant difference of methylation in the intron region between the SPSS- and decitabine-treated groups. On account of the lower level of p-mTOR, Th17

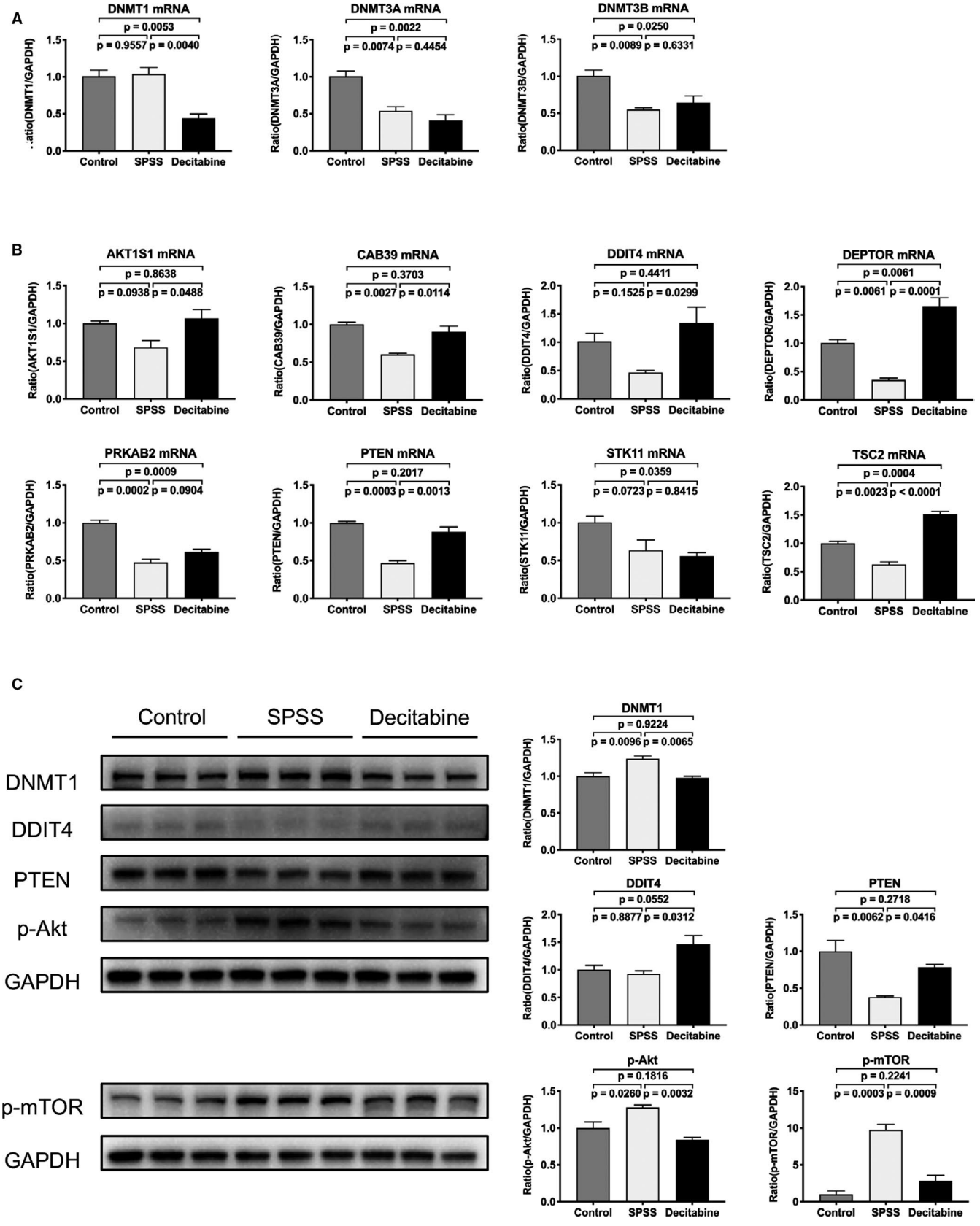

FIGURE 7 Activity of the mTOR signaling pathway was regulated by decitabine treatment. A, Quantitative PCR analysis of *Dnmt1/3a/3b* from recipient spleens on postoperative day 7. B, Quantitative PCR analysis of *Akt1s1*, *Cab39*, *Ddit4*, *Deptor*, *Prkab2*, *Pten*, *Stk11*, and *Tsc2* mRNA expression from the spleens of recipient mice. C, Western blot analysis of DNMT1, DDIT4, PTEN, p-Akt, and p-mTOR from the spleens. Data are expressed as the mean ± SEM. DDIT4, DNA damage inducible transcript 4; DNMT, DNA methyltransferase; mTOR, mechanistic target of rapamycin; PCR, polymerase chain reaction; PTEN, phosphatase and tensin homolog; SPSS, stroke-physiological saline solution.

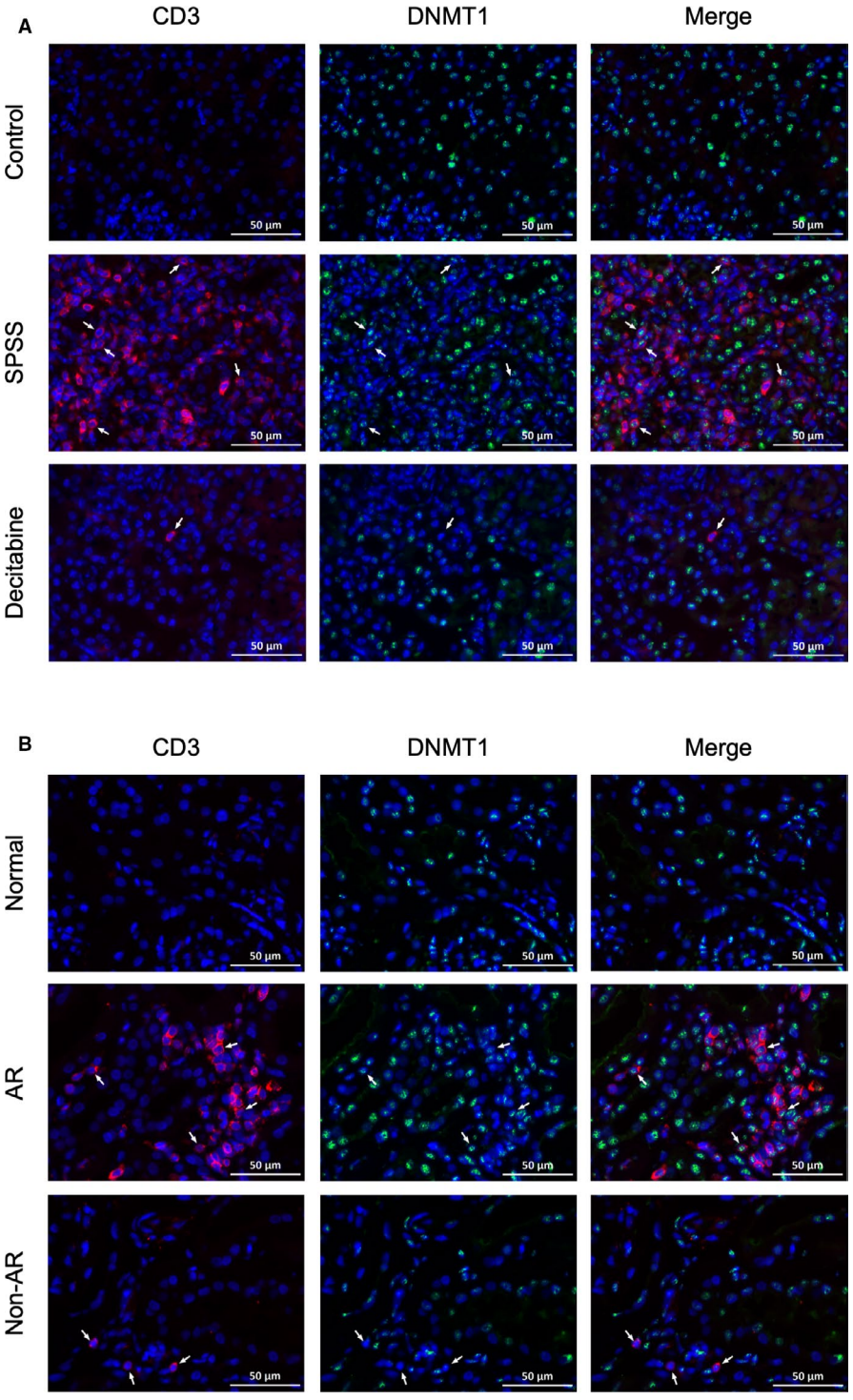

FIGURE 8 DNMT1-expressing $CD3^+$ T cells in recipients with acute rejection. A, Two-color immunofluorescence staining to identify T cells that co-express CD3 (Red) and DNMT1 (Green) markers in mouse grafted kidneys on postoperative day 7. B, Two-color immunofluorescence staining to identify T cells that co-express CD3 (Red) and DNMT1 (Green) markers in biopsy specimens from patients with no or a mild inflammatory response and acute rejection. Examples of $DNMT1^+CD3^+$ T cells are indicated by arrows. Nuclei were stained with DAPI (blue). Scale bar = 50 μm; AR, acute rejection; DNMT, DNA methyltransferase; SPSS, stroke-physiological saline solution

cells would be expected to be decreased; however, we found that the levels of Th17 cell-associated factors were elevated, which could be partially attributed to the specific microenvironment. Christian et al[27] found that naive T cells treated with decitabine induced RORC expression by demethylation of the *RORC* locus. Additionally, the increase of RORC may be due to the reduction in the *Foxp3* level, because TGF-β-induced *Foxp3* could antagonize RORC function.[42] Furthermore, a suppressed mTOR pathway also affects the cell cycle by promoting cell cycle inhibitors and inhibiting cyclin expression.[43-45]

Our results indicated that methylation plays a role in the mTOR signaling pathway and the subsequent alterations influenced the allograft fate, which was consistent with the findings of hypermethylated genes involved in mTOR signaling pathways in the AR-induced graft dysfunction group. These results therefore contribute new insight into the mechanisms of allograft rejection and dysfunction. Moreover, several studies indicated that the majority of genes with differentially methylated loci identified in the peripheral blood could be reflected in the kidney tissues.[25,46] Therefore, DNA methylation can serve as

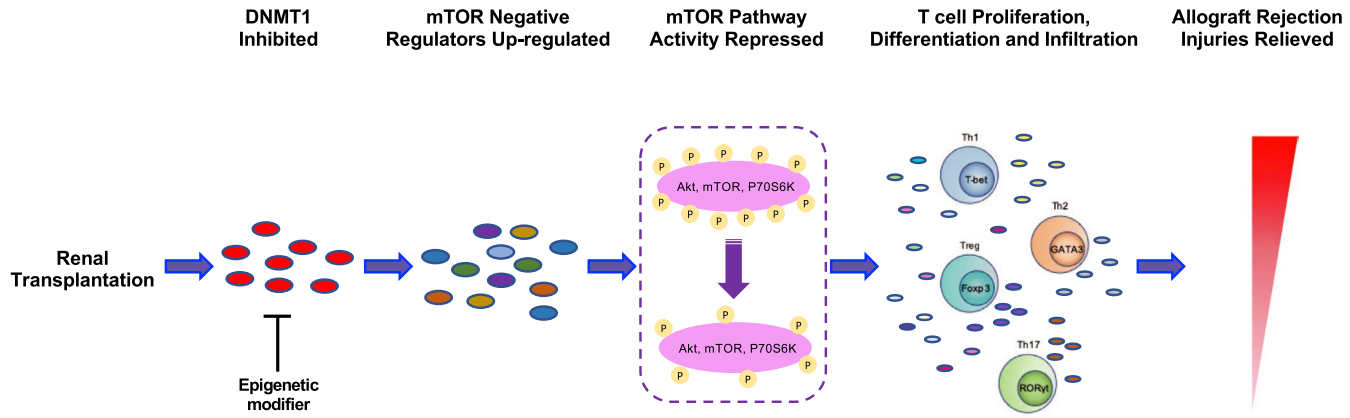

FIGURE 9 Summary of the mechanism of allograft survival involving the mTOR pathway regulated by DNA methylation. DNMT1 inhibits the expression of the mTOR upstream negative regulators to cause the phosphorylation of AKT, mTOR, and P70S6K, and ultimately influence the immune response. The DNA methylation inhibitor decitabine restrains the expression of DNMT1 and the high activity of mTOR pathway, ultimately ameliorating T cell–mediated rejection and improving the allograft survival. DNMT, DNA methyltransferase; mTOR, mechanistic target of rapamycin

a promising biomarker for predicting the outcome of transplanted kidneys. However, further studies are needed to confirm the specific advantage of methylation, as an early warning for AR-induced dysfunction after transplantation based on DNA methylation-regulated CpG sites.

In summary, this study provides a novel discovery that methylation modification occurred following the transplantation, with higher activity in the case of AR-induced allograft dysfunction, and the DNMT inhibitor decitabine alleviated allograft rejection in a mouse model by suppressing the activity of the mTOR pathway (Figure 9). These findings highlight the potential therapeutic benefits of epigenetic modifiers and provide new insights into the mechanism of transplant rejection and dysfunction offering strong evidence for further exploration.

DISCLOSURE

The authors of this manuscript have no conflicts of interest to disclose as described by the *American Journal of Transplantation*.

AUTHOR CONTRIBUTIONS

CZ and WX performed clinical data collection, the methylation microarray assay, flow cytometry, data analysis, and wrote the manuscript; BL and YW performed the mouse renal transplantation and revised the manuscript; SF analyzed flow cytometry results; CW performed the PCR and western blot assays. YC, BL, LQ, and HH collected patient blood; FA and AK prepared the library; SN and WX helped with DNA preparation and bisulfite conversion; SMMR and FN performed bioinformatics analyses; HJ conceived and supervised the study, designed and guided the experiments, and supervised the writing of the manuscript. JC offered clinical support; and all authors reviewed the manuscript.

DATA AVAILABILITY STATEMENT

All data relevant to this study are available from the corresponding author on reasonable request.

ORCID

Jianghua Chen https://orcid.org/0000-0002-3282-3998
Hong Jiang https://orcid.org/0000-0001-7692-5745

REFERENCES

1. Abecassis M, Bartlett ST, Collins AJ, et al. Kidney transplantation as primary therapy for end-stage renal disease: a National Kidney Foundation/Kidney Disease Outcomes Quality Initiative (NKF/KDOQITM) conference. *Clin J Am Soc Nephrol*. 2008;3(2):471-480.
2. Wolfe RA, Ashby VB, Milford EL, et al. Comparison of mortality in all patients on dialysis, patients on dialysis awaiting transplantation, and recipients of a first cadaveric transplant. *N Engl J Med*. 1999;341(23):1725-1730.
3. Kramer A, Pippias M, Noordzij M, et al. The European Renal Association - European Dialysis and Transplant Association (ERA-EDTA) Registry Annual Report 2015: a summary. *Clin Kidney J*. 2018;11(1):108-122.
4. Nankivell BJ, Alexander SI. Rejection of the kidney allograft. *N Engl J Med*. 2010;363(15):1451-1462.
5. Wu O, Levy AR, Briggs A, et al. Acute rejection and chronic nephropathy: a systematic review of the literature. *Transplantation*. 2009;87(9):1330-1339.
6. Meier-Kriesche HU, Schold JD, Srinivas TR, et al. Lack of improvement in renal allograft survival despite a marked decrease in acute rejection rates over the most recent era. *Am J Transplant*. 2004;4(3):378-383.
7. Tantravahi J, Womer KL, Kaplan B. Why hasn't eliminating acute rejection improved graft survival? *Annu Rev Med*. 2007;58:369-385.
8. He JC, Chuang PY, Ma'ayan A, et al. Systems biology of kidney diseases. *Kidney Int*. 2012;81(1):22-39.
9. Jiang S, Chuang PY, Liu ZH, et al. The primary glomerulonephritides: a systems biology approach. *Nat Rev Nephrol*. 2013;9(9):500-512.
10. Neusser MA, Lindenmeyer MT, Kretzler M, et al. Genomic analysis in nephrology–towards systems biology and systematic medicine? *Nephrol Ther*. 2008;4(5):306-311.
11. Dressler GR, Patel SR. Epigenetics in kidney development and renal disease. *Transl Res*. 2015;165(1):166-176.
12. Martinez SR, Gay MS, Zhang L. Epigenetic mechanisms in heart development and disease. *Drug Discov Today*. 2015;20(7):799-811.
13. Murrell A, Hurd PJ, Wood IC. Epigenetic mechanisms in development and disease. *Biochem Soc Trans*. 2013;41(3):697-699.

14. Rodriguez RM, Lopez-Larrea C, Suarez-Alvarez B. Epigenetic dynamics during CD4(+) T cells lineage commitment. *Int J Biochem Cell Biol*. 2015;67:75-85.
15. Jones PA. Functions of DNA methylation: islands, start sites, gene bodies and beyond. *Nat Rev Genet*. 2012;13(7):484-492.
16. Wu SC, Zhang Y. Active DNA demethylation: many roads lead to Rome. *Nat Rev Mol Cell Biol*. 2010;11(9):607-620.
17. Thomas RM, Gamper CJ, Ladle BH, et al. De novo DNA methylation is required to restrict T helper lineage plasticity. *J Biol Chem*. 2012;287(27):22900-22909.
18. Wu H, Zhang Y. Reversing DNA methylation: mechanisms, genomics, and biological functions. *Cell*. 2014;156(1–2):45-68.
19. Mas VR, Le TH, Maluf DG. Epigenetics in kidney transplantation: current evidence, predictions, and future research directions. *Transplantation*. 2016;100(1):23-38.
20. Hannum G, Guinney J, Zhao L, et al. Genome-wide methylation profiles reveal quantitative views of human aging rates. *Mol Cell*. 2013;49(2):359-367.
21. Horvath S. DNA methylation age of human tissues and cell types. *Genome Biol*. 2013;14(10):R115.
22. Dor Y, Cedar H. Principles of DNA methylation and their implications for biology and medicine. *Lancet*. 2018;392(10149):777-786.
23. Bestard O, Cunetti L, Cruzado JM, et al. Intragraft regulatory T cells in protocol biopsies retain foxp3 demethylation and are protective biomarkers for kidney graft outcome. *Am J Transplant*. 2011;11(10):2162-2172.
24. Bechtel W, McGoohan S, Zeisberg EM, et al. Methylation determines fibroblast activation and fibrogenesis in the kidney. *Nat Med*. 2010;16(5):544-550.
25. Smyth LJ, McKay GJ, Maxwell AP, et al. DNA hypermethylation and DNA hypomethylation is present at different loci in chronic kidney disease. *Epigenetics*. 2014;9(3):366-376.
26. Jones B, Chen J. Inhibition of IFN-gamma transcription by site-specific methylation during T helper cell development. *EMBO J*. 2006;25(11):2443-2452.
27. Schmidl C, Hansmann L, Andreesen R, et al. Epigenetic reprogramming of the RORC locus during in vitro expansion is a distinctive feature of human memory but not naive Treg. *Eur J Immunol*. 2011;41(5):1491-1498.
28. Hori S, Nomura T, Sakaguchi S. Control of regulatory T cell development by the transcription factor Foxp3. *Science*. 2003;299(5609):1057-1061.
29. Chen G, Chen H, Ren S, et al. Aberrant DNA methylation of mTOR pathway genes promotes inflammatory activation of immune cells in diabetic kidney disease. *Kidney Int*. 2019;96(2):409-420.
30. Kalina SL, Mottram PL. A microsurgical technique for renal transplantation in mice. *Aust N Z J Surg*. 1993;63(3):213-216.
31. Guo H, Wang W, Zhao NA, et al. Inhibiting cardiac allograft rejection with interleukin-35 therapy combined with decitabine treatment in mice. *Transpl Immunol*. 2013;29(1–4):99-104.
32. Morris TJ, Butcher LM, Feber A, et al. ChAMP: 450k chip analysis methylation pipeline. *Bioinformatics*. 2014;30(3):428-430.
33. Selvarajan V, Osato M, Nah GSS, et al. RUNX3 is oncogenic in natural killer/T-cell lymphoma and is transcriptionally regulated by MYC. *Leukemia*. 2017;31(10):2219-2227.
34. Wong WF, Kohu K, Chiba T, et al. Interplay of transcription factors in T-cell differentiation and function: the role of Runx. *Immunology*. 2011;132(2):157-164.
35. Lin FC, Liu YP, Lai CH, et al. RUNX3-mediated transcriptional inhibition of Akt suppresses tumorigenesis of human gastric cancer cells. *Oncogene*. 2012;31(39):4302-4316.
36. Kang KA, Kim KC, Bae SC, et al. Oxidative stress induces proliferation of colorectal cancer cells by inhibiting RUNX3 and activating the Akt signaling pathway. *Int J Oncol*. 2013;43(5):1511-1516.
37. Suarez-Alvarez B, Baragano Raneros A, Ortega F, et al. Epigenetic modulation of the immune function: a potential target for tolerance. *Epigenetics*. 2013;8(7):694-702.
38. Delgoffe GM, Pollizzi KN, Waickman AT, et al. The kinase mTOR regulates the differentiation of helper T cells through the selective activation of signaling by mTORC1 and mTORC2. *Nat Immunol*. 2011;12(4):295-303.
39. Lee K, Gudapati P, Dragovic S, et al. Mammalian target of rapamycin protein complex 2 regulates differentiation of Th1 and Th2 cell subsets via distinct signaling pathways. *Immunity*. 2010;32(6):743-753.
40. Wang YY, Jiang H, Wang YC, et al. Deletion of Smad3 improves cardiac allograft rejection in mice. *Oncotarget*. 2015;6(19):17016-17030.
41. Kim HP, Leonard WJ. CREB/ATF-dependent T cell receptor-induced FoxP3 gene expression: a role for DNA methylation. *J Exp Med*. 2007;204(7):1543-1551.
42. Zhou L, Lopes JE, Chong MM, et al. TGF-beta-induced Foxp3 inhibits T(H)17 cell differentiation by antagonizing RORgammat function. *Nature*. 2008;453(7192):236-240.
43. Zhang W, Lei C, Fan J, et al. miR-18a promotes cell proliferation of esophageal squamous cell carcinoma cells by increasing cyclin D1 via regulating PTEN-PI3K-AKT-mTOR signaling axis. *Biochem Biophys Res Commun*. 2016;477(1):144-149.
44. Chang H, Li J, Cao Y, et al. Bufadienolides from venenum bufonis inhibit mTOR-mediated Cyclin D1 and retinoblastoma protein leading to arrest of cell cycle in cancer cells. *Evid Based Complement Alternat Med*. 2018;2018:3247402.
45. Song J, Salek-Ardakani S, So T, et al. The kinases aurora B and mTOR regulate the G1-S cell cycle progression of T lymphocytes. *Nat Immunol*. 2007;8(1):64-73.
46. Ko Y-A, Mohtat D, Suzuki M, et al. Cytosine methylation changes in enhancer regions of core pro-fibrotic genes characterize kidney fibrosis development. *Genome Biol*. 2013;14(10):R108.

SUPPORTING INFORMATION

Additional supporting information may be found online in the Supporting Information section.

How to cite this article: Zhu C, Xiang W, Li B, et al. DNA methylation modulates allograft survival and acute rejection after renal transplantation by regulating the mTOR pathway. *Am J Transplant*. 2020;00:1–15. https://doi.org/10.1111/ajt.16183